https://www.scirp.org/journal/jbise
Journal of Biomedical Science and Engineering, 2026, Vol. 19, (No. 6), pp: 189-209

Development and Validation of a Vascular Flow Phantom for Doppler Ultrasound Evaluation

Millena Victoria Azevedo de Souza[1], Fernanda Vastag[1], Valéria Alves de Alencar[1], Henrique Zenga Carrenho[2], Marcia Roberta de Souza Caffeu[1], Luiz Carlos da Silva[1], Jônatas Cerqueira Dias[3], Jeferson Cerqueira Dias[1], Diolino José dos Santos Filho[2]

[1]Department of Biomedical Systems Technology, Faculty of Technology, Osasco, Brazil; [2]Department of Mechatronic and Mechanical Systems Engineering, University of São Paulo, São Paulo, Brazil; [3]Department of Information Technology, Faculty of Technology, Praia Grande, Brazil

Correspondence to: Jeferson Cerqueira Dias, jefersondias1@alumni.usp.br
Keywords: Phantom, Tissue-Mimicking Material, Doppler Ultrasound, Vascular Flow
Received: June 2, 2026 **Accepted:** June 12, 2026 **Published:** June 15, 2026

ABSTRACT

Vascular flow phantoms are essential tools for the calibration of Doppler ultrasound systems, professional training, and experimental hemodynamic studies. This study aimed to develop and validate a low-cost vascular flow phantom capable of reproducing clinically relevant blood flow patterns, including disturbed and non-laminar conditions, for Doppler ultrasound evaluation. The proposed system consists of tissue-mimicking materials, vessel-mimicking structures, a controlled hydraulic circuit, and an embedded electronic control system based on the ESP32 microcontroller. Metallic spheres were incorporated within the flow channel to generate controlled flow perturbations, enabling the simulation of complex hemodynamic scenarios. Experimental validation was performed using a ultrasound system with standardized acquisition parameters. The phantom successfully reproduced distinct flow regimes, including laminar and turbulent conditions. Quantitative Doppler measurements demonstrated clear differences between flow profiles, including spectral broadening and heterogeneous color flow patterns in regions with induced disturbances, supporting the reproducibility and functional reliability of the proposed system. The results indicate that the developed phantom is suitable for biomedical engineering research, ultrasound training, and functional validation of Doppler imaging systems. Its modular structure also enables future expansion for more complex cardiovascular simulations.

1. INTRODUCTION

Ultrasound phantoms are specially engineered physical models designed to simulate the mechanical and acoustic properties of biological tissues, vessels, and fluids. These models play an essential role in medical education, equipment calibration, quality assurance, and the validation of new diagnostic techniques, particularly in Doppler ultrasonography [1-3]. Their use allows the safe reproduction of clinical conditions without exposing patients to unnecessary procedures, while also enabling reproducible experimental studies under controlled laboratory conditions [4].

In recent years, the growing use of Doppler ultrasound in vascular diagnosis has increased the demand for reliable simulators capable of reproducing realistic hemodynamic conditions. Doppler ultrasonography is widely used for the assessment of blood flow velocity, direction, turbulence, and vascular abnormalities such as stenosis, reflux, and thrombosis [5, 6]. Consequently, the availability of robust and reproducible flow phantoms has become increasingly important for both professional training and technical validation of imaging systems [7].

Traditionally, tissue-mimicking materials such as gelatin, agar, and hydrogels have been widely used in phantom construction because of their acoustic similarity to soft tissues [8, 9]. Among these materials, polyvinyl alcohol (PVA)-based hydrogels have demonstrated versatility in different imaging applications. However, these materials often present important limitations, including dehydration, low long-term mechanical stability, susceptibility to microbial degradation, and reduced durability under repeated use conditions [10]. These constraints may compromise the reproducibility and lifespan of the phantom, particularly in dynamic flow simulations [11].

Alternative materials based on paraffin gel, mineral oil, and copolymer systems such as styrene-ethylene/butylene-styrene (SEBS) have emerged as promising solutions to overcome these limitations [12]. Previous studies have demonstrated favorable acoustic propagation speeds and attenuation coefficients in these materials, making them suitable for ultrasound applications [13]. Moreover, paraffin-based and silicone-based systems present improved durability, mechanical resistance, and cost-effectiveness, which are highly desirable characteristics for laboratory and educational use [14, 15].

Despite the significant advances reported in the literature, an important scientific and technological gap remains. Most currently available phantoms are limited either to static tissue simulation or to simplified vascular flow representations that do not adequately reproduce the diversity of clinically relevant hemodynamic patterns [16, 17]. In particular, there is a lack of low-cost, modular physical models capable of simulating multiple flow regimes, including laminar, pulsatile, intermittent, retrograde, and turbulent flow, while simultaneously allowing quantitative Doppler validation [18, 19].

This limitation directly affects the training of healthcare professionals, the calibration of ultrasound systems, and the development of new diagnostic methodologies. Furthermore, currently available models often do not include internal structures capable of generating controlled disturbances in the flow field, which are essential for evaluating turbulence, vessel obstruction, and imaging performance [20].

In addition, the growing need for accessible biomedical simulators reinforces the relevance of this study, particularly in environments where access to commercial solutions is limited [21, 22].

Therefore, this study aims to develop and experimentally validate a vascular flow phantom for Doppler ultrasound evaluation capable of reproducing multiple physiologically relevant hemodynamic patterns. The proposed system integrates tissue-mimicking materials, controlled fluid circulation, and internal markers for the generation of distinct flow behaviors, including laminar and turbulent regimes. The main objective is to provide a robust, accessible, and reproducible platform for Doppler ultrasound validation, professional training, and vascular research applications.

The central hypothesis of this work is that the integration of durable tissue-mimicking materials with a dynamically controlled vascular flow circuit can produce a realistic and quantitatively reliable phantom suitable for simulating clinically relevant Doppler conditions and improving diagnostic training and equipment validation.

The central hypothesis of this work is that the integration of durable tissue-mimicking materials with

a dynamically controlled vascular flow circuit can produce a realistic and quantitatively reliable phantom, suitable for simulating clinically relevant Doppler conditions and improving the quality of diagnostic training and equipment validation.

2. THEORETICAL FOUNDATION OR LITERATURE REVIEW

2.1. Ultrasound

Ultrasound (US) consists of mechanical waves with frequencies above the human audible threshold, typically ranging from approximately 20 kHz to several megahertz, depending on the diagnostic application [12, 13]. Over recent decades, technological advances have significantly expanded the clinical use of ultrasound, particularly in diagnostic imaging, where tissue properties such as density, attenuation, and acoustic impedance are translated into high-resolution images [13-15].

Clinical ultrasound systems are generally composed of a computer processing unit, monitor, and transducer, operating in the range of 2 - 15 MHz, depending on the anatomical structure under investigation [16]. The transducer contains piezoelectric elements that convert electrical excitation into acoustic waves and, subsequently, reflected echoes into electrical signals for image formation [17].

In vascular applications, Doppler ultrasound plays a central role because it enables the evaluation of flow direction, velocity, turbulence, and hemodynamic disturbances, which are essential for the diagnosis of vascular disorders and for calibration of simulation systems [4, 18]. This capability makes Doppler ultrasonography particularly suitable for validating vascular phantoms designed to reproduce physiological and pathological blood flow patterns.

Furthermore, portable ultrasound technologies have broadened access to diagnostic imaging in remote and emergency environments, reinforcing the need for accessible and reproducible calibration tools [11].

2.2. Ultrasound Phantoms and Tissue Simulation Materials

Ultrasound phantoms are physical models specifically designed to reproduce the mechanical, acoustic, and structural properties of biological tissues, allowing realistic simulation of clinical conditions without patient exposure [1-4]. These systems are widely used in:

- professional training
- equipment calibration
- validation of imaging systems
- development of novel diagnostic techniques

Several materials have been investigated for phantom construction, including:

- gelatin
- agar
- polyvinyl alcohol (PVA)
- silicone-based compounds
- SEBS copolymer gels

[8-10].

Among these, silicone-based materials and polymeric hydrogels stand out due to their durability, mechanical stability, and acoustic similarity to human soft tissues.

Recent studies have demonstrated that custom-made vascular phantoms significantly improve the quantitative validation of Doppler systems, especially in flow-based applications [2, 4, 23].

2.3. Clinical Relevance and Vascular Pathologies

The clinical relevance of vascular flow simulation is directly associated with the diagnosis and monitoring of several vascular disorders.

Pathological changes such as:

- stenosis

- aneurysms
- partial obstructions
- reflux
- arterial bifurcation disturbances

produce measurable changes in Doppler flow patterns [24-27].

Laminar flow represents physiological conditions, while turbulent and retrograde flows are frequently associated with clinically relevant abnormalities.

In particular, vascular bifurcations and narrowing regions are known to induce local turbulence and recirculation zones, which may contribute to endothelial dysfunction and atherosclerotic progression [24, 25].

Therefore, the development of vascular phantoms capable of reproducing these flow conditions is highly relevant for:

- medical education
- Doppler calibration
- experimental hemodynamic research

2.4. Blood Circulation and Vascularization

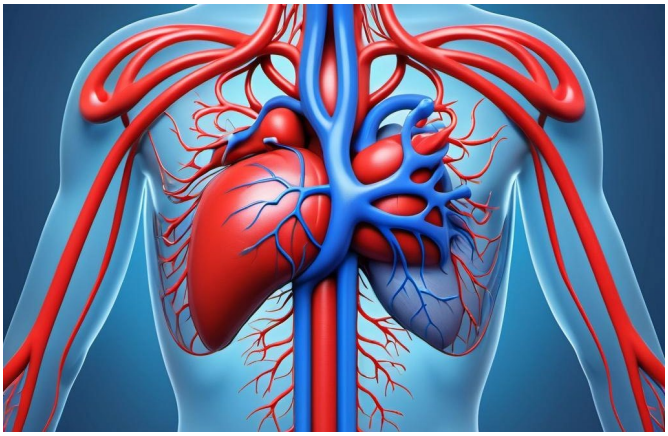

Source: Author, 2025.

Figure 1. Circulatory system animation.

The circulatory system, as shown in **Figure 1**, is composed of the heart and an extensive network of blood vessels, including arteries, veins, and capillaries, responsible for maintaining tissue perfusion and metabolic homeostasis [28].

The heart acts as a pulsatile pump that generates blood flow throughout the vascular network. Arteries transport oxygenated blood from the heart to tissues, whereas veins return deoxygenated blood and metabolic waste products.

This hemodynamic behavior serves as the physiological basis for the design of the proposed phantom system.

The simulation of this vascular environment is essential for reproducing clinically relevant Doppler signals.

2.5. Blood Flow Patterns and Their Pathological Implications

Blood flow patterns may be classified as:

- laminar
- pulsatile

- intermittent
- retrograde
- turbulent

[24-27].

Laminar flow is characterized by organized fluid layers moving in parallel, with minimal internal disturbance.

Turbulent flow, in contrast, is associated with abrupt velocity changes, eddy formation, and non-uniform flow distribution.

Pulsatile flow is typical of arterial circulation and reflects the cyclic systolic and diastolic phases of cardiac activity.

Retrograde flow is commonly observed in vascular insufficiency and obstruction syndromes.

Understanding these flow regimes is essential for the interpretation of Doppler signals and for the development of realistic calibration phantoms.

This theoretical basis directly supports the experimental flow conditions tested in the Results section.

2.6. Risk Management and Device Validation Framework (ISO 14971:2019)

This subsection was completely revised to align with the study theme.

In accordance with ISO 14971:2019, the development of medical simulation devices and calibration tools requires systematic risk assessment throughout the product lifecycle [29].

For the present vascular phantom, risk management principles were considered during:

- material selection
- hydraulic design
- electrical control
- Doppler validation
- experimental reproducibility

Particular attention was given to:

- leakage prevention
- electrical safety of the control system
- stability of flow generation
- repeatability of Doppler measurements
- safe use in academic and laboratory environments

The application of ISO 14971 strengthens the reliability and safety of the proposed system while supporting future translational use for calibration and educational applications.

3. MATERIALS AND METHODS

This study is classified as applied experimental research, as it aims to provide a practical solution to an existing problem in biomedical engineering and medical imaging validation [24, 25, 30]. The methodological approach combined bibliographic review, experimental development, and laboratory validation procedures, integrating material preparation, hydraulic circuit design, electronic control, and Doppler ultrasound assessment [24, 25].

The development of the phantom simulator involved the definition of a base material and the selection of components capable of reproducing vascularized soft tissue structures, including vessels, bifurcations, and flow disturbances [26, 27]. The proposed methodology was designed to simulate multiple hemodynamic patterns relevant to Doppler ultrasonography, including laminar and turbulent flow conditions.

3.1. Block Diagram of the Phantom Flow for Doppler Ultrasound

Figure 2 illustrates the block diagram of the developed Phantom Flow system for vascular Doppler ultrasound simulation. The system consists of a closed-loop hydraulic circuit in which the pump drives the blood-mimicking fluid through the phantom structure, reproducing different hemodynamic conditions.

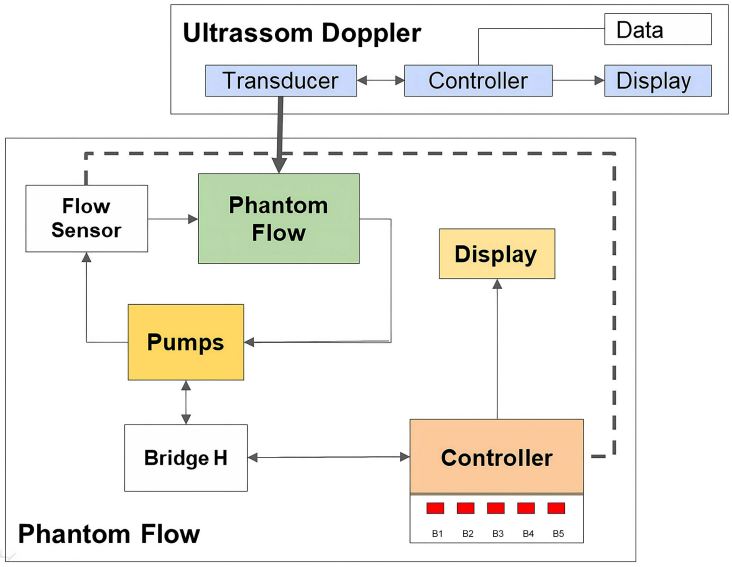

Source: Author, 2025.

Figure 2. Block Diagram of the Phantom Flow for Doppler Ultrasound

The flow sensor continuously monitors the fluid flow rate and transmits the signal to the electronic controller, which adjusts the pump performance through an H-bridge-based control system. A display module allows real-time visualization of the selected flow condition and operational parameters.

The Doppler ultrasound transducer captures fluid movement inside the phantom, transmitting the reflected signals to the SIEMENS ACUSON NX3 system for image formation and velocity analysis. This modular architecture enables synchronized interaction between mechanical flow generation and ultrasound diagnostic response, supporting both educational and research applications [26].

3.2. Soft Tissue Mimicking Material (TMM)

Source: Author, 2025.

Figure 3. Soft Tissue-Mimicking Material (TMM)

For the fabrication of the tissue-mimicking material (TMM) as shown in **Figure 3**, Ecoflex 00–30 (Smooth-On, Inc.) was selected due to its suitable balance between acoustic performance and mechanical stability, especially for supporting microchannels and bifurcated vascular structures [2].

The preparation procedure followed the original experimental protocol: a mold with dimensions of 6 × 5 × 3 cm was used, with an internal opening positioned approximately 10 mm from the bottom to allow

formation of the branched vascular phantom.

For the final phantom dimensions of 5.5 × 5 × 2.5 cm, 50 mL of silicone mixture was used, combined with approximately 0.15 g of cellulose (Sigma Aldrich) to act as an ultrasound scattering agent. After vigorous homogenization, the mixture was degassed in a vacuum chamber at −762 mmHg for 10 minutes to remove microbubbles and then cured for approximately 3 hours [2, 8-10].

3.3. Blood-Mimicking Material (BMM)

According to Kim *et al.* [23], glycerin was selected as the primary component of the blood-mimicking material due to its ability to modulate acoustic and rheological properties according to concentration.

The fluid was prepared by mixing:

- 50 g of 99% glycerin
- 500 g of deionized water

resulting in a 10% glycerin concentration.

The mixture was stirred at 650 rpm for 30 minutes using a mechanical agitator to ensure complete homogenization [31].

This formulation was chosen to simulate flow viscosity and Doppler reflectivity similar to physiological blood flow conditions.

3.4. Vessel-Mimicking Material (VMM)

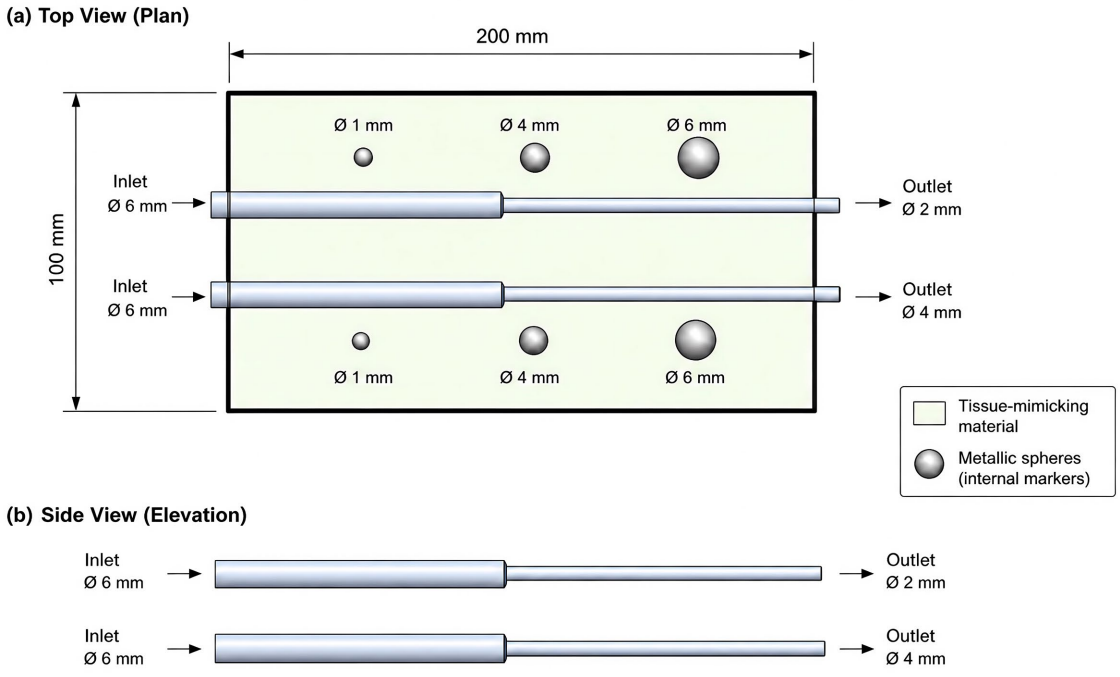

Note: Dimensions are in millimeters (mm). The scales of the diameters are not proportional.

Source: Author, 2025.

Figure 4. Vessel-Mimicking Material (VMM).

The vascular structure was fabricated using polyvinyl alcohol (PVA) through 3D printing technology, following the methodology adapted from Laughlin *et al.* [31].

As illustrated in **Figure 4**, the phantom incorporates two parallel vessel channels with controlled geometric variations. Each vessel presents an inlet diameter of 6 mm, followed by a gradual reduction to outlet

diameters of 2 mm (upper vessel) and 4 mm (lower vessel), respectively. This configuration enables the simulation of different flow regimes associated with vessel narrowing and diameter transitions, which are commonly observed in physiological and pathological vascular conditions.

The bifurcated and cylindrical vessel geometries were manufactured using a MakerBot Replicator 2X extrusion printer under the following conditions:

- extruder temperature: 185˚C
- print bed temperature: 60˚C

Additionally, metallic spheres with diameters of 1 mm, 4 mm, and 6 mm were strategically embedded within the tissue-mimicking material surrounding the vessels, as shown in the top view (**Figure 4(a)**). These internal markers act as controlled flow disturbance elements, promoting localized variations in velocity, recirculation zones, and turbulence.

The combined effect of vessel diameter reduction and the presence of embedded spherical markers allows the phantom to reproduce both laminar and disturbed flow conditions, thereby enhancing its applicability for Doppler ultrasound calibration and for the investigation of hemodynamic responses under clinically relevant scenarios [26].

3.5. Electrical Circuit Diagram

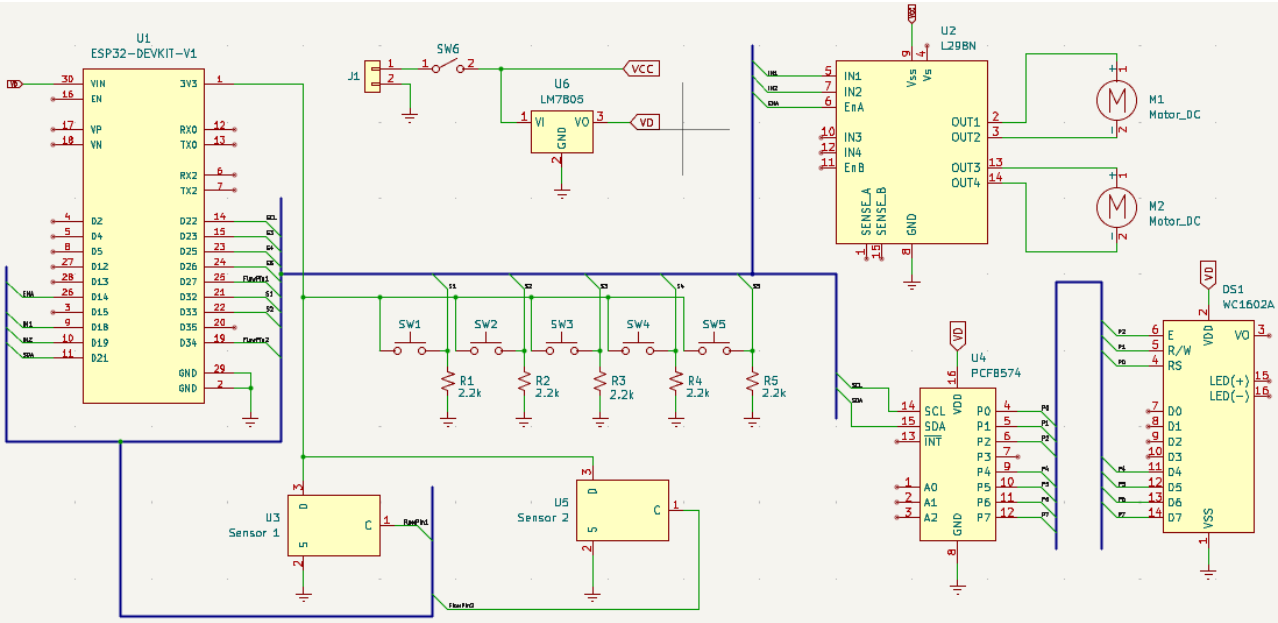

Source: Author, 2025.

Figure 5. Electrical circuit diagram.

The electrical circuit, as showing in **Figure 5**, was developed using the ESP32-DEVKIT-V1 platform to enable controlled generation of multiple flow regimes within the experimental phantom. The system integrates two DC motor-driven pumps, corresponding flow sensors, a 12 V power supply, an LM7805 voltage regulator, and an L298N H-bridge motor driver.

Unlike conventional motor control circuits, the proposed architecture allows the generation of five distinct and reproducible flow patterns through discrete control inputs (SW1 - SW5), combining pump activation, flow direction control, and speed modulation. This configuration enables the simulation of different hemodynamic conditions, including steady, pulsatile, and turbulent flow regimes.

The 12 V supply directly powered the pumps, while the LM7805 provided regulated 5 V voltage for sensitive electronic components. The L298N module enabled both speed control and bidirectional rotation

control, ensuring precise adjustment of flow patterns and allowing simulation of flow direction changes relevant to Doppler ultrasound analysis [32].

Additionally, the integration of dual flow sensors provides real-time monitoring of the generated flow, supporting validation and repeatability of the experimental conditions.

Embedded Control Algorithm and ESP32 Programming

The control logic of the hydraulic phantom system was implemented using the ESP32-DEVKIT-V1 microcontroller platform, programmed within the Arduino IDE environment according to the code presented in Table 1, which is widely adopted in experimental prototyping and biomedical instrumentation studies [32-34].

The embedded software architecture was designed to ensure accurate and reproducible control of the hemodynamic conditions generated within the phantom. The developed code performs the following core functions:

- control of the peristaltic pump rotation speed through PWM modulation
- activation and synchronization of the auxiliary pump
- real-time acquisition of flow sensor signals
- signal processing and conversion into volumetric flow rate
- real-time data visualization via the display interface

The system continuously reads the pulse output generated by the flow sensors and converts it into flow rate values using a previously calibrated conversion factor, ensuring measurement consistency under different experimental conditions [33, 35].

The general flow calculation is expressed as:

$$Q = \frac{N}{k} \cdot t \tag{1}$$

where:

Q = flow rate

N = number of pulses counted

k = sensor calibration constant

t = acquisition time interval

Additionally, the control algorithm regulates pump actuation via the L298N H-bridge driver, allowing dynamic adjustment of flow intensity and direction. This capability is essential for reproducing physiologically relevant flow regimes, such as laminar, pulsatile, and turbulent patterns.

The software structure was modularly organized into:

- initialization routine
- sensor acquisition loop
- flow computation module
- display update routine
- pump control logic

This embedded control strategy ensures system stability, repeatability, and synchronization between hydraulic flow generation and Doppler signal acquisition, which are critical requirements for experimental validation in biomedical engineering applications [32, 34, 35].

Table 1. Table with ESP32 programming code for the phantom flow.

Nrline	Code	Nr line	Code
1	#include <Wire.h>	18	unsigned long currentTime;
2	#include <LiquidCrystal_I2C.h>	19	unsigned long elapsedTime;
3	#define PWM_PIN 14 // botão do motor, pino ENB	20	//int sensor;

Continued

```
#define pino1 18// pino do motor, pino in3
#define pino2 19 // pino do motor, pino in4
#define botao1 32
#define botao2 33
#define botao3 23
#define botao4 25
#define botao5 26
#define flowPin1 27
#define flowPin2 34
volatile uint32_t pulseCount = 0;
float flowRate = 0.0;    // Litros por minuto
float totalLiters = 0.0;    // Acumulado em litros
float flowLiters = 0.0;
unsigned long lastTime;
void sensor()
{
currentTime = millis();
elapsedTime = currentTime - lastTime;
if (elapsedTime >= 1000)
{
// A cada 1 segundo
detachInterrupt(flowPin1); // Evita conflito ao ler a variável
// Cálculo da vazão (L/min)
//flowRate = (pulseCount / 7.5);
// Volume que passou no último segundo
flowLiters = (pulseCount *60 / 5880.0); // Convertido para Litros por segundo, conta pulso durante 1 segundo, miultiplica por 60 segundos, e divide por 5880, conforme o manual do sensor para dar 1 L
//totalLiters += flowLiters;
lcd.setCursor(0,1);
lcd.print("Vazao: ");
LiquidCrystal_I2Clcd(0x27,16,2
int tempo;
unsigned long tempo_anterior;
unsigned long tempo_atual;
const int frequencia=500;
const int resolucao=8;
const int canal = 0;
int dutycycle = 50;
void IRAM_ATTR countPulse()
{
pulseCount += 1;
}
void sensor()
{
pinMode(pino1, OUTPUT);
pinMode(pino2, OUTPUT);
ledcAttachChannel(PWM_PIN,frequencia,resolucao,canal);
Serial.begin(115200);
pinMode(botao1, INPUT);
pinMode(botao2, INPUT);
pinMode(botao3, INPUT);
pinMode(botao4, INPUT);
pinMode(botao5, INPUT);
pinMode(flowPin1, INPUT_PULLUP);
attachInterrupt(flowPin1, countPulse, countPulse, RISING);RISING);
lastTime = millis();
pulseCount = 0;
void loop()
sensor();
```

Continued

```
50  lcd.setCursor(7,1);
51  lcd.print(flowLiters);
52  lcd.setCursor(11,1);
53  //Serial.print(flowRate);
54  lcd.print(" L/min");
55  //Serial.print("Total: ");
56  //Serial.print(totalLiters, 3);
57  //Serial.println(" L");
58  pulseCount = 0;
59  lastTime = currentTime;
60  attachInterrupt(flowPin1, countPulse, RISING);
61  void setup()
62  lcd.init();                    // initialize the lcd
63  lcd.backlight();
64  lcd.setCursor(0,0);
65  lcd.print("PHANTOM DOPPLER ");
66  pinMode(PWM_PIN,OUTPUT);
82  if(digitalRead(botao1)==HIGH)
83  sensor();
84  lcd.setCursor(0,0);
85  lcd.print("                    ");
86  lcd.setCursor(0,0);
87  lcd.print("Intermitente");
88  tempo = 5000;
89  digitalWrite(pino1, HIGH);
90  digitalWrite(pino2, LOW);
91  for (int i =0; i<=2;i++)
92  ledcFade(PWM_PIN,153,255,tempo);
93  digitalWrite(pino1, HIGH);
94  digitalWrite(pino2, LOW);
95  //delay(tempo);
96  tempo_anterior=millis();
97  tempo_atual=millis();
98  while(tempo_atual-tempo_anterior <= tempo)
99  tempo_atual=millis();
100 sensor();
101 digitalWrite(pino1, LOW);
102 digitalWrite(pino2, LOW);
103 ledcFade(PWM_PIN,255,153,tempo);
104 digitalWrite(pino1, HIGH);
105 digitalWrite(pino2, LOW);
106 //delay(tempo);
107 tempo_anterior=millis();
108 tempo_atual=millis();
109 while(tempo_atual-tempo_anterior <= tempo)
110 tempo_atual=millis();
111 sensor();v
112 // Fluxo turbulento= começa com 40% vai para 100%, vai para 60% e termina em 80%
113 if(digitalRead(botao2)==HIGH)
114 sensor();
133 tempo_atual=millis();
134 sensor();
135 if(digitalRead(botao3)==HIGH)
136 sensor()
137 lcd.setCursor(0,0);
138 lcd.print("                    ");
139 lcd.setCursor(0,0);
140 lcd.print("Laminar");
141 dutycycle=153;
142 ledcWrite(PWM_PIN, dutycycle);
143 digitalWrite(pino1, HIGH);
144 digitalWrite(pino2, LOW);
145 //Fluxo retrogrado = começa com 80% e permane nesse valor, porém muda o sentido/
146 if(digitalRead(botao4)==HIGH)
147 sensor();
148 lcd.setCursor(0,0);
```

Continued

```
115 lcd.setCursor(0,0);
116 lcd.print("                ");
117 lcd.setCursor(0,0);
118 lcd.print("Turbulento");
119 digitalWrite(pino2, LOW);
120 tempo=10000;
121 ledcFade(PWM_PIN,102,255,tempo);
122 //delay(tempo);
123 tempo_anterior=millis();
124 tempo_atual=millis();
125 while(tempo_atual-tempo_anterior <= tempo)
126 tempo_atual=millis();
127 sensor();
128 ledcFade(PWM_PIN,153,204,tempo);
129 //delay(tempo);
130 tempo_anterior=millis();
131 tempo_atual=millis();
132 while(tempo_atual-tempo_anterior <= tempo)
167 for (int i=0;i<= 2;i++)
168 ledcFade(PWM_PIN,0,255,temo);
169 tempo_anterior=millis();
170 tempo_atual=millis();
171 while(tempo_atual-tempo_anterior <= tempo)
172 tempo_atual=millis();
173 sensor();
174 //delay (tempo);
175 tempo_anterior=millis();
176 tempo_atual=millis();
149 lcd.print("                ");
150 lcd.setCursor(0,0);
151 lcd.print("Retrogrado");
152 dutycycle=204;
153 ledcWrite(PWM_PIN, dutycycle);
154 digitalWrite(pino1, LOW);
155 digitalWrite(pino2, HIGH);
156 if(digitalRead(botao5)==HIGH)
157 sensor();
158 /*dutycycle=255;Fluxo pulsado , o tempo está em segundos= 12000milisegundos = 12 segundos
159 ledcWrite(PWM_PIN, dutycycle);*/
160 lcd.setCursor(0,0);
161 lcd.print("                ");
162 lcd.setCursor(0,0);
163 lcd.print("Pulsado");
164 digitalWrite(pino1, HIGH);
165 digitalWrite(pino2, LOW);
166 tempo = 10000;
177 while(tempo_atual-tempo_anterior <= tempo)
178 tempo_atual=millis();
179 sensor();
180 ledcFade(PWM_PIN,255,0,tempo);
181 //delay (tempo);
182 tempo_anterior=millis();
183 tempo_atual=millis();
184 while(tempo_atual-tempo_anterior <= tempo)
185 tempo_atual=millis();
186 sensor();
```

Continuous reading of the buttons allows the code to adjust the rotation speed of the motors in real time using pulse width modulation (PWM). This precise control is essential for faithfully simulating hemodynamic conditions in training and research environments, particularly in experimental biomedical systems that require repeatability and stability [32, 34].

In the main loop, the code logic automatically cycles through the flow descriptions every 2 seconds on

the display while monitoring the button states. When a button press is detected, the microcontroller computes the corresponding motor speed and activates the system accordingly. Otherwise, the motors remain off, ensuring operational safety and energy efficiency, in line with recommended practices for embedded system reliability [36].

The use of commands such as analogWrite() (for PWM-based motor control), digitalRead() (for input acquisition), and lcd.setCursor() / lcd.print() (for display output) enables direct hardware interfacing, contributing to system responsiveness and efficiency.

This simple yet robust programming approach allows the ESP32 to function as a central control unit for biomedical simulation, providing flexibility, reproducibility, and reliable operation across different experimental scenarios [33].

3.6. AutoCAD Project Diagram

The AutoCAD project diagram of the Phantom Flow and Control System, shown in **Figure 6**, illustrates a hemodynamic simulation setup designed for testing and calibration of Doppler ultrasound systems [24]. The system consists of two cylindrical reservoirs (R1 and R2), each with a volume of 3 liters, containing fluids that simulate venous blood (blue) and arterial blood (red), respectively. These fluids circulate continuously through a closed-loop system and return to their respective reservoirs.

The system incorporates two peristaltic pumps (B1 and B2), each with a flow rate of 4.5 L/min, responsible for driving the fluid from the reservoirs through the circuit. The pumps are connected via flexible tubing, enabling continuous and controlled fluid circulation. Each pump is monitored by a flow sensor (S1 and S2), allowing real-time tracking of flow conditions. The pumps are controlled by an ESP32-based microcontroller, which enables the configuration of up to five distinct flow profiles—linear, intermittent, pulsatile, turbulent, and retrograde—thus simulating a range of clinically relevant hemodynamic conditions.

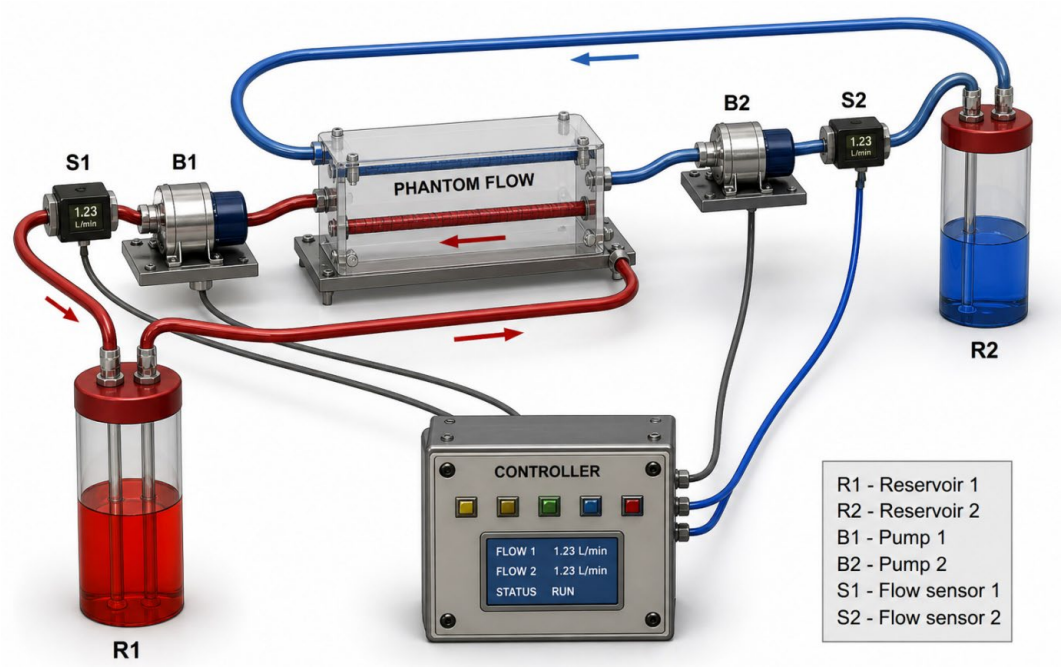

Source: Author, 2025.

Figure 6. **Dynamic phantom flow design.**

Selection and adjustment of flow profiles are performed through five control buttons, while system status and operational parameters are displayed on an LCD interface. The electronic control circuit is

powered by a 12 V supply, ensuring system portability and stable operation during experimental procedures.

The fluid driven by the pumps circulates through the vascular phantom, represented by polyvinyl alcohol (PVA) tubes with diameters of 8 mm and 4 mm, allowing the investigation of different vessel geometries and flow velocities [32, 33]. These vessels are embedded within a tissue-mimicking material composed of silicone (polydimethylsiloxane) crosslinked with a platinum catalyst, providing acoustic properties compatible with ultrasound propagation.

To enhance Doppler signal analysis, metallic spheres with diameters of 30 mm, 20 mm, 10 mm, 2 mm, and 1 mm were incorporated into the phantom structure. These inclusions act as controlled flow disturbance elements, promoting localized variations in velocity and enabling the evaluation of Doppler sensitivity under conditions such as partial obstruction, flow acceleration, and turbulence, as reported in experimental phantom studies [29, 32].

The overall assembly was designed to support detailed investigation of simulated blood flow behavior and its interaction with internal structures, providing a reliable and reproducible platform for calibration, validation, and training applications in Doppler ultrasound.

3.7. Testing and Validation of the Phantom with Doppler Ultrasound

The phantom testing was conducted in a laboratory environment using a VF 10-5 linear transducer operating at a frequency of 6.2 MHz, which is suitable for imaging superficial vascular structures [16]. Initially, the B-mode (2D) imaging was activated, followed by the color Doppler mode to enable visualization of flow dynamics within the phantom. The thyroid preset was selected due to its optimization for small- and medium-caliber vessels.

During the experiments, key Doppler parameters—including gain, operating frequency, pulse repetition frequency (PRF), and wall filters—were adjusted to optimize flow visualization and signal quality. These parameters are known to directly influence Doppler sensitivity, resolution, and artifact suppression [13, 18]. The configuration enabled clear distinction of simulated flow patterns, represented by red and blue color mapping corresponding to flow direction relative to the transducer [4].

Technical parameters were carefully tuned to balance spatial resolution, sensitivity, and image stability. The PRF was maintained at 1563 Hz, appropriate for moderate flow velocities and avoiding aliasing artifacts [18]. The wall filter was set to a low level to allow detection of low-velocity flows without excessive noise interference.

Additional system settings included color priority (Priority 4), smoothing (Smooth 2), and medium flow mode (Flow M), which contributed to improved visualization stability. The frame rate was fixed at 13 frames per second, ensuring adequate temporal resolution without compromising image quality.

The lateral color bar provided a reference for interpreting flow direction and relative velocity, while thermal and mechanical indices remained within safe operational limits, in accordance with standard ultrasound safety practices [13].

4. RESULTS AND DISCUSSION

The developed vascular flow phantom demonstrated satisfactory structural integrity and functional performance during all experimental validation stages. The system was capable of reproducing distinct hemodynamic flow patterns, including laminar and turbulent flow regimes, allowing qualitative and quantitative assessment through Doppler ultrasound imaging under controlled laboratory conditions. The experimental setup, described in Section 3.7, was tested using a VF 10-5 linear transducer operating at 6.2 MHz, with a pulse repetition frequency (PRF) of 1563 Hz and frame rate of 13 fps, ensuring appropriate sensitivity and image stability for superficial vascular simulation.

4.1. Quantitative Doppler Analysis under Turbulent Flow Conditions

Figure 7 presents the color Doppler image obtained during the turbulent flow simulation using the

SIEMENS ACUSON NX3 device. The region of interest (ROI), highlighted in green, clearly defines the hemodynamic analysis zone within the vascular phantom. A mixed chromatic distribution, including red, orange, blue, and green transitions, was observed, which is characteristic of disturbed and non-uniform flow behavior.

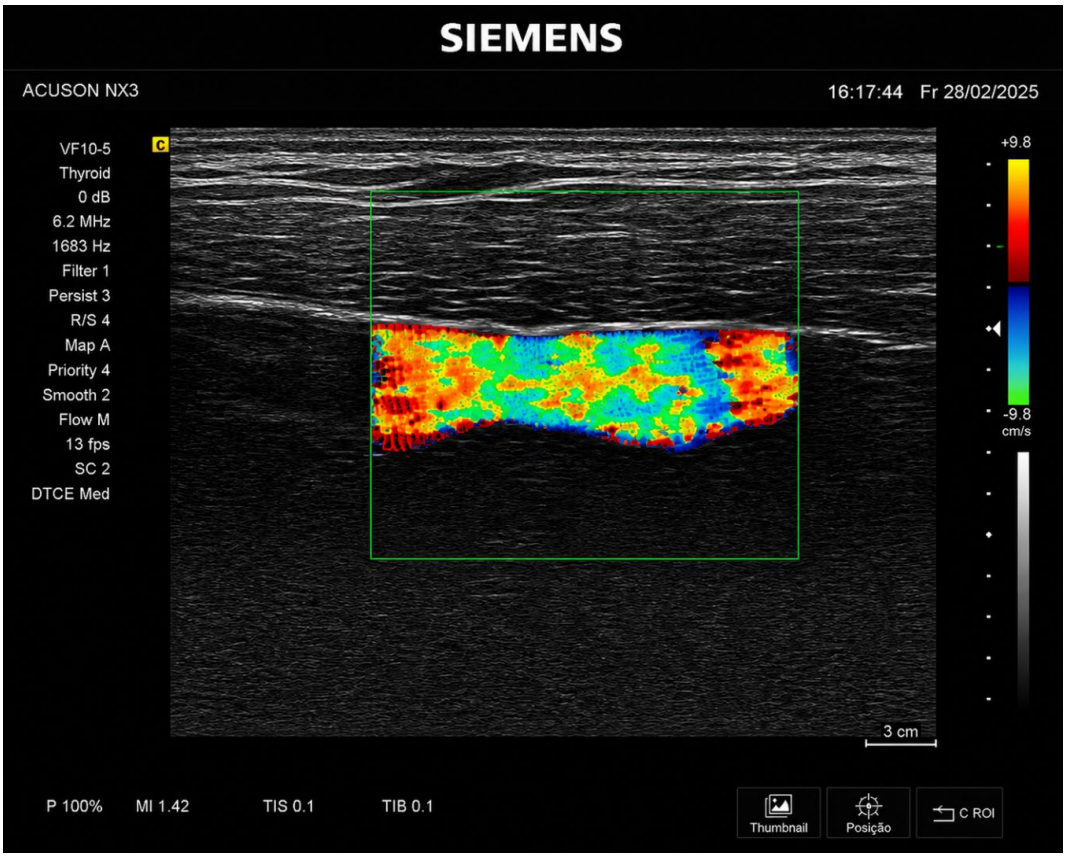

Source: Author, 2025.

Figure 7. Color Doppler ultrasound - color box - mix color - turbulence flow.

The Doppler lateral scale indicated a **maximum measured velocity of 9.8 cm/s**, corresponding to the turbulent regime induced by the internal metallic markers positioned inside the vessel lumen. This increased velocity, combined with color aliasing and chromatic inversion, confirms the successful generation of localized turbulence, simulating clinically relevant conditions such as vascular stenosis, bifurcation disturbances, and flow recirculation zones [25, 26].

The presence of these flow disturbances demonstrates that the proposed phantom is capable of reproducing pathological hemodynamic conditions relevant for Doppler ultrasound training, experimental validation, and calibration of imaging systems [24, 29].

4.2. Quantitative Doppler Analysis under Left Laminar Flow Conditions

Figure 8 shows the color Doppler result obtained during the simulation of stable leftward laminar flow. A uniform blue coloration was observed throughout the vascular lumen, indicating a unidirectional flow moving away from the transducer, with no evidence of turbulence, reflux, or recirculation.

The measured velocity was 5.9 cm/s, which is compatible with controlled physiological laminar flow simulation. The vessel walls remained sharply delineated, and no artifacts associated with bubbles, flow instability, or interference from the embedded markers were identified.

These findings confirm the stability of the hydraulic circuit and validate the performance of pump B1 and the microcontroller-based control system. The flow profile is consistent with physiological arterial or venous laminar flow conditions described in the literature [25, 28].

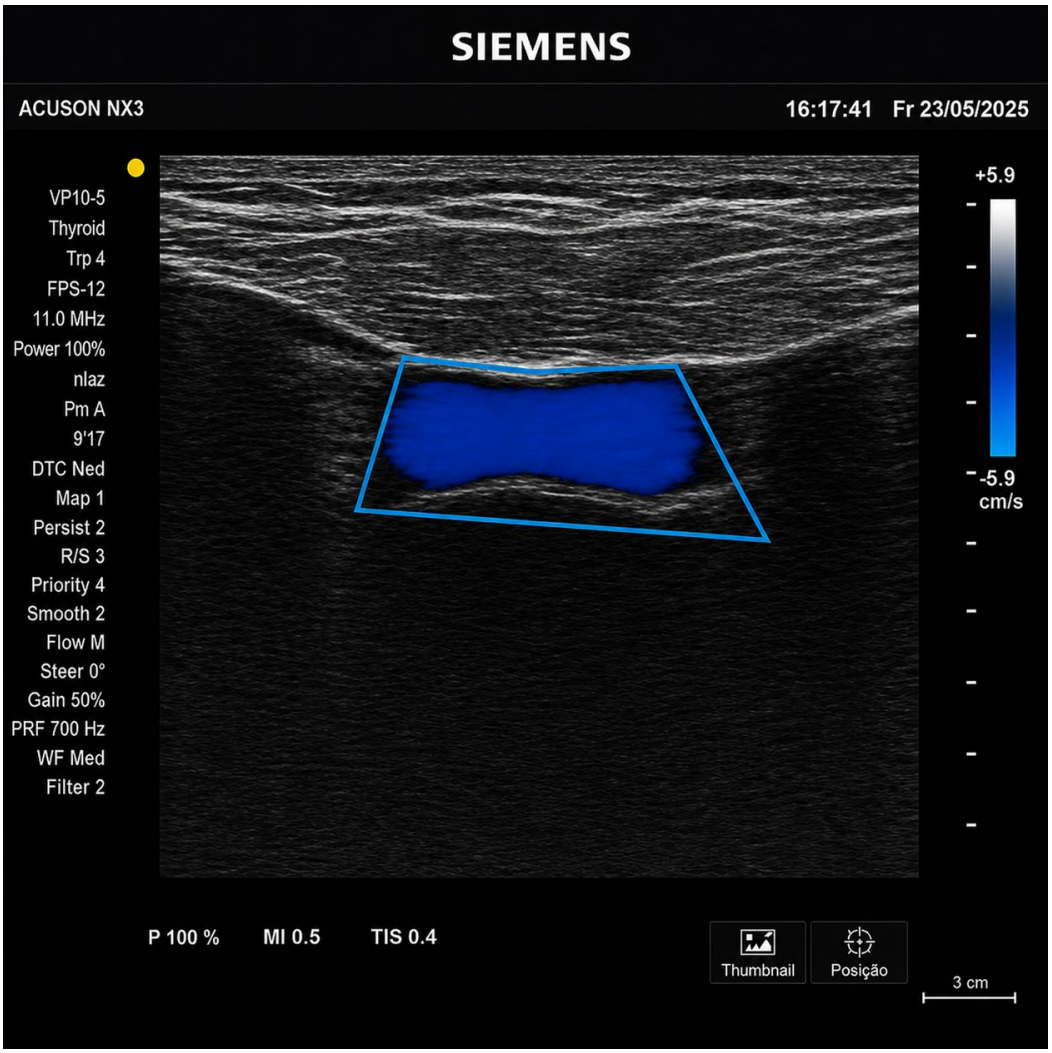

Source: Author, 2025.

Figure 8. Color Doppler ultrasound - color box - blue.

4.3. Quantitative Doppler Analysis under Right Laminar Flow Conditions

Figure 9 presents the Doppler ultrasound image corresponding to the rightward laminar flow simulation. In this condition, a homogeneous red coloration was observed, indicating flow toward the transducer.

The measured velocity was 6.1 cm/s, which is very close to the value obtained in the left laminar flow condition, demonstrating high symmetry and repeatability of the developed phantom.

The difference between both laminar flow conditions was:

$$\Delta V = 6.1 - 5.9 = 0.2\,\text{cm/s} \tag{2}$$

This corresponds to a relative difference of:

$$\Delta V(\%) = \frac{0.2}{5.9} \times 100 = 3.39\% \tag{3}$$

A deviation of only 3.39% indicates excellent reproducibility of the system and robust calibration of both hydraulic branches.

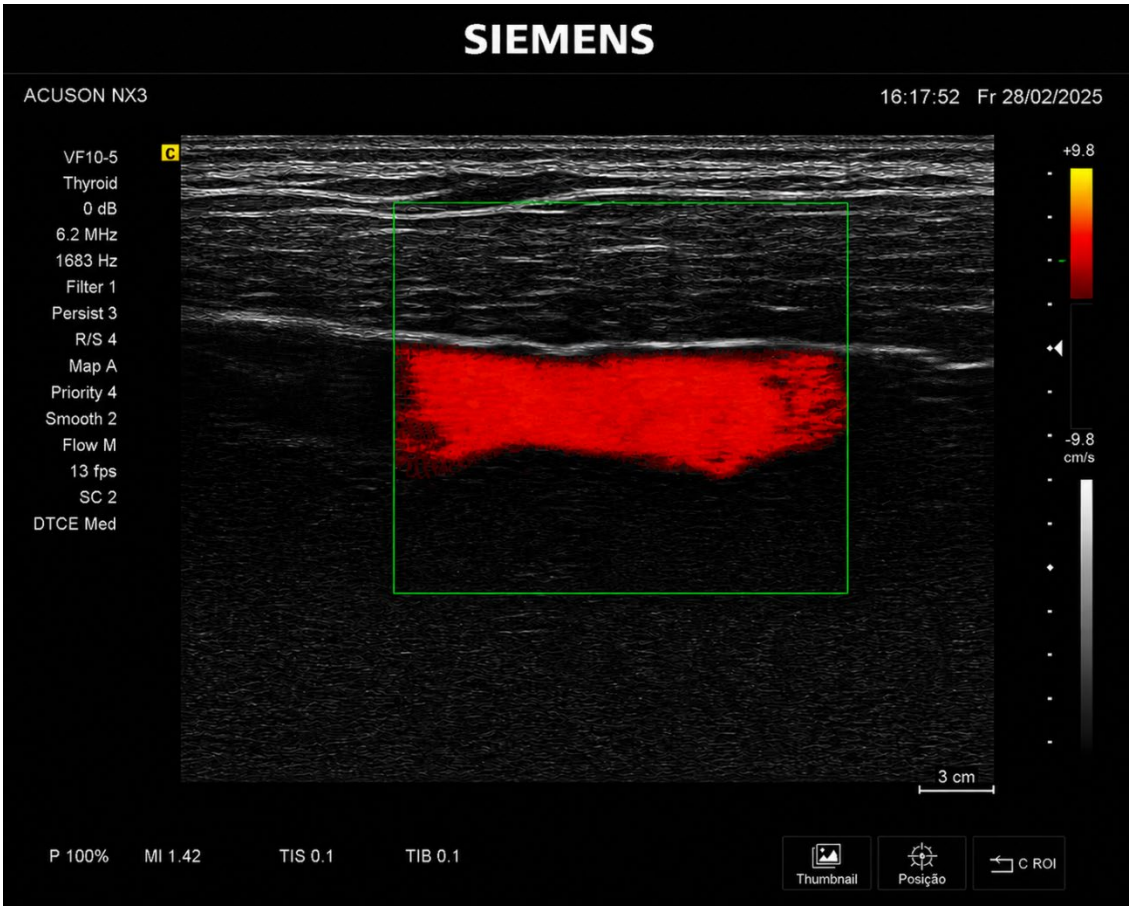

Source: Author, 2025.

Figure 9. Color Doppler ultrasound - color box - red.

4.4. Comparative Quantitative Performance

To improve the objective presentation of the results, the main quantitative outputs are summarized in Table 2.

Table 2. Quantitative Doppler performance of the vascular flow phantom.

Flow Condition	Velocity (cm/s)	Flow Pattern	Stability	Clinical Simulation
Left laminar flow	5.9	Uniform blue	High	Physiological flow
Right laminar flow	6.1	Uniform red	High	Physiological flow
Turbulent flow	9.8	Mixed colors	Moderate	Stenosis / disturbed flow

The turbulent flow condition showed a significant increase in velocity compared to the left laminar flow condition, calculated as:

$$\Delta V = \frac{9.8 - 5.9}{5.9} \times 100 = 66.1\% \quad (4)$$

Thus, the turbulent condition produced an approximate 66.1% increase in flow velocity, quantitatively confirming the effectiveness of the internal disturbance elements in generating non-uniform and clinically relevant hemodynamic conditions [25, 27, 36].

This result is consistent with expected flow behavior in regions of vascular narrowing and bifurcation, where increased velocity and turbulence are commonly observed due to flow acceleration and instability [27, 28].

4.5. Experimental Interpretation and Performance Discussion

From an engineering perspective, the developed phantom demonstrated stable hydraulic and acoustic behavior throughout all experimental tests. The tissue-mimicking material maintained adequate acoustic propagation properties, ensuring consistent ultrasound signal transmission, while the blood-mimicking fluid enabled reliable Doppler signal acquisition under different flow regimes [2, 8, 19].

The system successfully reproduced both physiological and pathological flow patterns, including laminar and turbulent conditions, confirming its capability to simulate clinically relevant hemodynamic scenarios [4, 36].

This performance reinforces the practical applicability of the proposed system for:

- Doppler ultrasound calibration
- biomedical engineering research
- academic and professional training [23, 32]
- controlled clinical simulation environments

Overall, these findings directly support the main objective of this study, demonstrating that the proposed low-cost vascular phantom provides a reliable, reproducible, and versatile platform for Doppler ultrasound evaluation and experimental validation.

5. CONCLUSIONS

The present study successfully developed and experimentally validated a vascular flow phantom for Doppler ultrasound evaluation, integrating tissue-mimicking materials, vessel-mimicking structures, a controlled hydraulic circuit, and an embedded electronic control and monitoring system.

Unlike conventional phantom designs, the proposed system enables the generation of multiple and reproducible flow regimes through an integrated microcontroller-based architecture, allowing controlled simulation of laminar, turbulent, pulsatile, intermittent, and retrograde flow patterns. This capability represents an important advancement by enabling systematic investigation of Doppler responses under distinct and clinically relevant hemodynamic conditions.

The experimental results demonstrated clear qualitative and quantitative differentiation between flow regimes. In particular, the incorporation of velocity measurements and comparative analysis confirmed the ability of the phantom to reproduce flow disturbances associated with clinically relevant conditions such as stenosis, bifurcation effects, and recirculation zones. The observed increase in velocity under turbulent conditions further supports the effectiveness of the internal disturbance elements embedded within the phantom.

Additionally, the inclusion of internal markers (metallic spheres) proved to be a valuable feature for inducing controlled flow perturbations, enabling enhanced evaluation of Doppler sensitivity, signal variation, and image response to localized disturbances. This aspect addresses a common limitation in simplified phantom models and strengthens the applicability of the system for both research and calibration purposes.

From an engineering perspective, the system demonstrated stable hydraulic performance, reliable electronic control, and consistent acoustic behavior, ensuring reproducibility of experimental conditions. The integration of real-time flow monitoring further contributes to the robustness and repeatability of the proposed methodology.

The results indicate that the developed phantom constitutes a reliable, accessible, and cost-effective platform for:

- Doppler ultrasound calibration
- biomedical engineering research
- professional and academic training
- experimental validation of imaging systems

Furthermore, the modular architecture allows future expansion toward more complex cardiovascular simulations, including variable vessel geometries, advanced pulsatile profiles, and patient-specific flow conditions.

Therefore, the proposed system represents a relevant scientific and technological contribution to the development of low-cost, flexible, and experimentally robust vascular phantoms, addressing current limitations in Doppler ultrasound validation and supporting advances in diagnostic imaging and training methodologies.

ACKNOWLEDGEMENTS

I would like to thank the CPRJI/CPS for the constant clarifications regarding the progress of the work, the Coordination of the Industrial Automation Course for the resources provided, and the management of the Osasco unit for their warm reception.

CONFLICTS OF INTEREST

The authors declare no conflicts of interest regarding the publication of this paper.

REFERENCES

1. Fučík, R., Galabov, R., Pauš, P., Eichler, P., Klinkovský, J., Straka, R., *et al.* (2020) Investigation of Phase-Contrast Magnetic Resonance Imaging Underestimation of Turbulent Flow through the Aortic Valve Phantom: Experimental and Computational Study Using Lattice Boltzmann Method. *Magnetic Resonance Materials in Physics, Biology and Medicine*, **33**, 649-662. https://doi.org/10.1007/s10334-020-00837-5
2. Adusei, S., Ternifi, R., Fatemi, M. and Alizad, A. (2023) Custom-Made Flow Phantoms for Quantitative Ultrasound Microvessel Imaging. *Ultrasonics*, **134**, Article ID: 107092. https://doi.org/10.1016/j.ultras.2023.107092
3. Hoferer, I., Jourdain, L., Girot, C., Benatsou, B., Leguerney, I., Cournede, P., *et al.* (2023) New Calibration Setup for Quantitative DCE-US Imaging Protocol: Toward Standardization. *Medical Physics*, **50**, 5541-5552. https://doi.org/10.1002/mp.16362
4. Dakok, K.K., Matjafri, M.Z., Suardi, N., Oglat, A.A. and Nabasu, S.E. (2021) A Review of Carotid Artery Phantoms for Doppler Ultrasound Applications. *Journal of Medical Ultrasound*, **29**, 157-166. https://doi.org/10.4103/jmu.jmu_164_20
5. Capellini, K., Ait-Ali, L., Pak, V., Cantinotti, M., Murzi, M., Vignali, E., *et al.* (2024) Three-Dimensional Printed Models as an Effective Tool for the Management of Complex Congenital Heart Disease. *Frontiers in Bioengineering and Biotechnology*, **12**. https://doi.org/10.3389/fbioe.2024.1369514
6. Cheng, A., Guo, X., Zhang, H.K., Kang, H.J., Etienne-Cummings, R. and Boctor, E.M. (2017) Active Phantoms: A Paradigm for Ultrasound Calibration Using Phantom Feedback. *Journal of Medical Imaging*, **4**, Article ID: 035001. https://doi.org/10.1117/1.jmi.4.3.035001
7. Shen, C., Lyu, L., Wang, G. and Wu, J. (2019) A Method for Ultrasound Probe Calibration Based on Arbitrary Wire Phantom. *Cogent Engineering*, **6**, Article ID: 1592739. https://doi.org/10.1080/23311916.2019.1592739
8. Madsen, E.L., Hobson, M.A., Shi, H., Varghese, T. and Frank, G.R. (2005) Tissue-Mimicking Agar/Gelatin Materials for Use in Heterogeneous Elastography Phantoms. *Physics in Medicine and Biology*, **50**, 5597-5618. https://doi.org/10.1088/0031-9155/50/23/013

9. Pavan, T.Z., Madsen, E.L., Frank, G.R., Jiang, J., Carneiro, A.A.O. and Hall, T.J. (2012) A Nonlinear Elasticity Phantom Containing Spherical Inclusions. *Physics in Medicine and Biology*, **57**, 4787-4804. https://doi.org/10.1088/0031-9155/57/15/4787

10. Bontempi, L., Zattoni, M., Ramella, A., Migliavacca, F., Ringgaard, S., Kim, W.Y., *et al.* (2025) Idealized Aortic Annuloplasty FSI Digital Twin of 3d-Printed Phantoms with 4d-Flow MRI Comparison. *Computers in Biology and Medicine*, **192**, 110398. https://doi.org/10.1016/j.compbiomed.2025.110398

11. Iniewski, K. (2012) Biological and Medical Sensor Technologies. CRC Press.

12. Hobbie, R. and Roth, B.J. (2007) Intermediate Physics for Medicine and Biology. Springer.

13. Carovac, A., Smajlovic, F. and Junuzovic, D. (2011) Application of Ultrasound in Medicine. *Acta Informatica Medica*, **19**, 168-171. https://doi.org/10.5455/aim.2011.19.168-171

14. Schmid-Wendtner, M. and Dill-Müller, D. (2008) Ultrasound Technology in Dermatology. *Seminars in Cutaneous Medicine and Surgery*, **27**, 44-51. https://doi.org/10.1016/j.sder.2008.01.003

15. Elmer, K.M., Caffin, C., Scott, B., Stephens, S.E. and Jensen, M.O. (2025) Development and Characteristics of a Dual-Layered Vascular Phantom. *Cardiovascular Engineering and Technology*, **17**, 25-40. https://doi.org/10.1007/s13239-025-00810-0

16. Abu-Zidan, F., Hefny, A. and Corr, P. (2011) Clinical Ultrasound Physics. *Journal of Emergencies, Trauma, and Shock*, **4**, 501-503. https://doi.org/10.4103/0974-2700.86646

17. Christensen, D. (1988) Ultrasonic Bioinstrumentation. Wiley.

18. Papaléo, R.M. and De Souza, D.S. (2019) Ultrassonografia: Princípios Físicos e Controle da Qualidade. *Revista Brasileira de Física Médica*, **13**, 14-23. https://doi.org/10.29384/rbfm.2019.v13.n1.p14-23

19. Vieira, S.L., Pavan, T.Z., Junior, J.E. and Carneiro, A.A.O. (2013) Paraffin-Gel Tissue-Mimicking Material for Ultrasound-Guided Needle Biopsy Phantom. *Ultrasound in Medicine & Biology*, **39**, 2477-2484. https://doi.org/10.1016/j.ultrasmedbio.2013.06.008

20. Movahed, M. (2007) Interference of Breast Implants with Echocardiographic Image Acquisition and Interpretation. *Cardiovascular Ultrasound*, **5**, Article No. 9. https://doi.org/10.1186/1476-7120-5-9

21. Honer, J.S. and McGough, R.J. (2025) Fast and Accurate Plane Wave and Color Doppler Imaging with the FOCUS Software Package. *Sensors*, **25**, 4276. https://doi.org/10.3390/s25144276

22. Lai, P., Xu, X. and Wang, L.V. (2014) Dependence of Optical Scattering from Intralipid in Gelatin-Gel Based Tissue-Mimicking Phantoms on Mixing Temperature and Time. *Journal of Biomedical Optics*, **19**, 035002. https://doi.org/10.1117/1.jbo.19.3.035002

23. Kim, N., Hong, C., Lee, C. and Cho, H. (2023) Development and Evaluation of Doppler Ultrasound Training Phantom for Human Vessel Simulation. *Applied Sciences*, **13**, 9932. https://doi.org/10.3390/app13179932

24. Oliveira, J.R.D., Aquino, M.D.A., Barros, S., Pitta, G.B.B. and Pereira, A.H. (2016) Alterations of Blood Flow Pattern after Triple Stent Endovascular Treatment of Saccular Abdominal Aortic Aneurysm: A Porcine Model. *Revista do Colégio Brasileiro de Cirurgiões*, **43**, 154-159. https://doi.org/10.1590/0100-69912016003004

25. Pinto, L.T.M., Januário, J.R., Nogueira, C.S., *et al.* (2021) Análise CFD do escoamento no interior da bifurcação da carótida. *Revista Interdisciplinar de Pesquisa em Engenharia*, **2**, 143-158.

26. Ishii, T., Takabe, S., Yanagawa, Y., Ohshima, Y., Kagawa, Y., Shibata, A., *et al.* (2019) Laser Doppler Blood Flowmeter as a Useful Instrument for the Early Detection of Lower Extremity Peripheral Arterial Disease in Hemodialysis Patients: An Observational Study. *BMC Nephrology*, **20**, 470. https://doi.org/10.1186/s12882-019-1653-y

27. Araújo, A.F., *et al.* (2021) Síndrome do roubo de subclávia. FHEMIG.

28. Sherwood, L. (2011) Fundamentals of Physiology. Thomson.
29. (2019) ISO 14971:2019, Medical Devices—Risk Management. ISO.
30. Calas, M.J.G., Koch, H.A. and Dutra, M.V.P. (2007) Ultra-sonografia mamária: Avaliação dos critérios ecográficos na diferenciação das lesões mamárias. *Radiologia Brasileira*, **40**, 1-7. https://doi.org/10.1590/s0100-39842007000100003
31. Laughlin, M.E., Stephens, S.E., Hestekin, J.A. and Jensen, M.O. (2021) Development of Custom Wall-Less Cardiovascular Flow Phantoms with Tissue-Mimicking Gel. *Cardiovascular Engineering and Technology*, **13**, 1-13. https://doi.org/10.1007/s13239-021-00546-7
32. Dias, J.C., Souza, M.V.A.D., Dias, J.C., Silva, L.C.D. and Filho, D.J.D.S. (2025) Development and Implementation of a Project Using Iomt Technology for Monitoring, Remote Control, and Tracking of a Left Ventricular Assist Device: Reduction of Adverse Events Caused by Malfunction Leading to Critical and Catastrophic Failures. *Journal of Biomedical Science and Engineering*, **18**, 250-261. https://doi.org/10.4236/jbise.2025.186018
33. Reiss, N., Schmidt, T., Boeckelmann, M., Schulte-Eistrup, S., Hoffmann, J., Feldmann, C., *et al.* (2018) Telemonitoring of Left-Ventricular Assist Device Patients—current Status and Future Challenges. *Journal of Thoracic Disease*, **10**, S1794-S1801. https://doi.org/10.21037/jtd.2018.01.158
34. Saeed, D., Feldman, D., Banayosy, A.E., *et al.* (2023) The 2023 International Society for Heart and Lung Transplantation Guidelines for Mechanical Circulatory Support: A 10-Year Update. *The Journal of Heart and Lung Transplantation*, **42**, e1-e222.
35. Phuttharak, J. and Loke, S.W. (2023) An Event-Driven Architectural Model for Integrating Heterogeneous Data and Developing Smart City Applications. *Journal of Sensor and Actuator Networks*, **12**, 12. https://doi.org/10.3390/jsan12010012
36. Rapp, E.S., Pawar, S.R. and Longoria, R.G. (2022) Hybrid Mock Circulatory Loop Simulation of Extreme Cardiac Events. *IEEE Transactions on Biomedical Engineering*, **69**, 2883-2892. https://doi.org/10.1109/tbme.2022.3156963